REPORT DOCUMENTATION PAGE

Form Approved OMB NO. 0704-0188

1. REPORT DATE (DD-MM-YYYY)	2. REPORT TYPE	3. DATES COVERED (From - To)
	New Reprint	-

4. TITLE AND SUBTITLE

Consequences of Anode Interfacial Layer Deletion. HCl-Treated ITO in P3HT:PCBM-Based Bulk-Heterojunction Organic Photovoltaic Devices

5a. CONTRACT NUMBER
W911NF-05-1-0177

5b. GRANT NUMBER

5c. PROGRAM ELEMENT NUMBER
611102

6. AUTHORS

Michael D. Irwin, Jun Liu, Benjamin J. Leever, Jonathan D. Servaites, Mark C. Hersam, Michael F. Durstock, and Tobin J. Marks

5d. PROJECT NUMBER

5e. TASK NUMBER

5f. WORK UNIT NUMBER

7. PERFORMING ORGANIZATION NAMES AND ADDRESSES

Northwestern University Chicago Campus
Office of Sponsored Research
Northwestern University
Evanston, IL 60208 -1110

8. PERFORMING ORGANIZATION REPORT NUMBER

9. SPONSORING/MONITORING AGENCY NAME(S) AND ADDRESS(ES)

U.S. Army Research Office
P.O. Box 12211
Research Triangle Park, NC 27709-2211

10. SPONSOR/MONITOR'S ACRONYM(S)
ARO

11. SPONSOR/MONITOR'S REPORT NUMBER(S)
48138-CH-PCS.9

12. DISTRIBUTION AVAILIBILITY STATEMENT

Approved for public release; federal purpose rights

13. SUPPLEMENTARY NOTES

The views, opinions and/or findings contained in this report are those of the author(s) and should not contrued as an official Department of the Army position, policy or decision, unless so designated by other documentation.

14. ABSTRACT

In studies to simplify the fabrication of bulk-heterojunction organic photovoltaic (OPV) devices, it was found that when glass/tin-doped indium oxide (ITO) substrates are treated with dilute aqueous HCl solutions, followed by UV-ozone (UVO), and then used to fabricate devices of the structure glass/ITO/P3HT:PCBM/LiF/Al, device performance is greatly enhanced. Light-to-power conversion efficiency (Eff) increases from 2.4% for control devices in which the ITO surface is treated only with UVO, to 3.8% with the HCl + UVO treatment – effectively

15. SUBJECT TERMS

conductive atomic force microscopy, indium tin oxide, organic photovoltaic

16. SECURITY CLASSIFICATION OF:			17. LIMITATION OF ABSTRACT	15. NUMBER OF PAGES	19a. NAME OF RESPONSIBLE PERSON
a. REPORT	b. ABSTRACT	c. THIS PAGE			Mark Hersam
UU	UU	UU	UU		19b. TELEPHONE NUMBER: 847-491-2696

Report Title

Consequences of Anode Interfacial Layer Deletion. HCl-Treated ITO in P3HT:PCBM-Based Bulk-Heterojunction Organic Photovoltaic Devices

ABSTRACT

In studies to simplify the fabrication of bulk-heterojunction organic photovoltaic (OPV) devices, it was found that when glass/tin-doped indium oxide (ITO) substrates are treated with dilute aqueous HCl solutions, followed by UV-ozone (UVO), and then used to fabricate devices of the structure glass/ITO/P3HT:PCBM/LiF/Al, device performance is greatly enhanced. Light-to-power conversion efficiency (Eff) increases from 2.4% for control devices in which the ITO surface is treated only with UVO, to 3.8% with the HCl + UVO treatment – effectively matching the performance of an identical device having a PEDOT:PSS anode interfacial layer. The enhancement originates from increases in VOC from 463 mV to 554 mV, and FF from 49% to 66%. The modified-ITO device also exhibits a 4x enhancement in thermal stability versus an identical device containing a PEDOT:PSS anode interfacial layer. To understand the origins of these effects, the ITO surface is analyzed as a function of treatment by ultraviolet photoelectron spectroscopy work function measurements, X-ray photoelectron spectroscopic composition analysis, and atomic force microscopic topography and conductivity imaging. Additionally, a diode-based device model is employed to further understand the effect of ITO surface treatment on device performance.

REPORT DOCUMENTATION PAGE (SF298)
(Continuation Sheet)

Continuation for Block 13

ARO Report Number 48138.9-CH-PCS
Consequences of Anode Interfacial Layer Deleti ...

Block 13: Supplementary Note

Approved for public release; federal purpose rights

Langmuir Article

pubs.acs.org/Langmuir

Consequences of Anode Interfacial Layer Deletion. HCl-Treated ITO in P3HT:PCBM-Based Bulk-Heterojunction Organic Photovoltaic Devices

Michael D. Irwin,[†] Jun Liu,[†] Benjamin J. Leever,[†,‡,§] Jonathan D. Servaites,[‡] Mark C. Hersam,*[,†,‡] Michael F. Durstock,[§] and Tobin J. Marks*[,†,‡]

[†]*Department of Chemistry, the Materials Research Center, and the Argonne Northwestern Solar Energy Research Institute, Northwestern University, 2145 Sheridan Road, Evanston, Illinois 60208-3113,* [‡]*Department of Materials Science and Engineering, Northwestern University, 2220 Campus Drive, Evanston, Illinois 60208-3108, and* [§]*Air Force Research Laboratory, Wright-Patterson AFB, Ohio 45433*

Received August 4, 2009. Revised Manuscript Received November 9, 2009

In studies to simplify the fabrication of bulk-heterojunction organic photovoltaic (OPV) devices, it was found that when glass/tin-doped indium oxide (ITO) substrates are treated with dilute aqueous HCl solutions, followed by UV ozone (UVO), and then used to fabricate devices of the structure glass/ITO/P3HT:PCBM/LiF/Al, device performance is greatly enhanced. Light-to-power conversion efficiency (*Eff*) increases from 2.4% for control devices in which the ITO surface is treated only with UVO to 3.8% with the HCl + UVO treatment−effectively matching the performance of an identical device having a PEDOT:PSS anode interfacial layer. The enhancement originates from increases in V_{OC} from 463 to 554 mV and *FF* from 49% to 66%. The modified-ITO device also exhibits a 4× enhancement in thermal stability versus an identical device containing a PEDOT:PSS anode interfacial layer. To understand the origins of these effects, the ITO surface is analyzed as a function of treatment by ultraviolet photoelectron spectroscopy work function measurements, X-ray photoelectron spectroscopic composition analysis, and atomic force microscopic topography and conductivity imaging. Additionally, a diode-based device model is employed to further understand the effects of ITO surface treatment on device performance.

I. Introduction

Organic photovoltaic (OPV) devices are of great interest due to their promise as low-cost alternatives to conventional inorganic photovoltaic devices, such as those based on Si, with the potential to be produced on a large scale by established high-throughput manufacturing methods, including roll-to-roll processing or screen printing.[1−16] While a significant research effort has focused on the active layer electron donor and acceptor materials, optimization of the device interfaces presents an equally important challenge which, most significantly, is generic to any OPV device architecture.[17−20] Interfacial phenomena that dictate device performance, such as Ohmic contacts, interfacial cohesion, and charge traps, are largely independent of the cell design but must specifically accommodate the particular donor and acceptor materials being employed. The broad applicability of interfacial tailoring for OPV function therefore merits detailed investigation. This approach has already proven successful in other organic electronic devices such as field-effect transistors (OFETs)[21−27] and light-emitting diodes (OLEDs),[28−38] and is now being evaluated

*Corresponding author. E-mail: t-marks@northwestern.edu.

(1) Benson-Smith, J. J.; Nelson, J. *Ser. Photoconvers. Sol. Energy* **2008**, *3*, 453−501.
(2) Brabec, C. J.; Durrant, J. R. *MRS Bull.* **2008**, *33* (7), 670−675.
(3) Coakley, K. M.; Liu, Y.; Goh, C.; McGehee, M. D. *MRS Bull.* **2005**, *30* (1), 37−40.
(4) Dennler, G.; Lungenschmied, C.; Neugebauer, H.; Sariciftci, N. S.; Labouret, A. *J. Mater. Res.* **2005**, *20* (12), 3224−3233.
(5) Gaudiana, R.; Brabec, C. *Nat. Photonics* **2008**, *2* (5), 287−289.
(6) Gledhill, S. E.; Scott, B.; Gregg, B. A. *J. Mater. Res.* **2005**, *20* (12), 3167−3179.
(7) Gratzel, M. *MRS Bull.* **2005**, *30* (1), 23−27.
(8) Guenes, S.; Neugebauer, H.; Sariciftci, N. S. *Chem. Rev. (Washington, DC, U.S.)* **2007**, *107* (4), 1324−1338.
(9) Kroon, R.; Lenes, M.; Hummelen, J. C.; Blom, P. W. M.; de Boer, B. *Polym. Rev. (Philadelphia, PA, U.S.)* **2008**, *48* (3), 531−582.
(10) Lira-Cantu, M.; Krebs, F. C. *Recent Res. Dev. Appl. Phys.* **2005**, *8*, 71−98.
(11) Morton, O. *Nature (London, U.K.)* **2006**, *443* (7107), 19−22.
(12) Shaheen, S. E.; Ginley, D. S.; Jabbour, G. E. *MRS Bull.* **2005**, *30* (1), 10−19.
(13) Shevaleevskiy, O. *Pure Appl. Chem.* **2008**, *80* (10), 2079−2089.
(14) Sun, S.-S.; Zhang, C. *Opt. Sci. Eng.* **2008**, *133*, 401−420.
(15) Thompson, B. C.; Frechet, J. M. J. *Angew. Chem., Int. Ed.* **2008**, *47* (1), 58−77.
(16) Tobjork, D.; Aarnio, H.; Makela, T.; Osterbacka, R. *Mater. Res. Soc. Symp. Proc.* **2008**, *1091E*, 1091-AA05-45.
(17) Moliton, A.; Nunzi, J.-M. *Polym. Int.* **2006**, *55* (6), 583−600.
(18) Rand, B. P.; Burk, D. P.; Forrest, S. R. *Phys. Rev. B: Condens. Matter Mater. Phys.* **2007**, *75* (11), 115327/1−115327/11.
(19) Irwin, M. D.; Buchholz, D. B.; Hains, A. W.; Chang, R. P. H.; Marks, T. J. *Proc. Natl. Acad. Sci. U.S.A.* **2008**, *105* (8), 2783−2787.
(20) Derouiche, H.; Djara, V. *Sol. Energy Mater. Sol. Cells* **2007**, *91* (13), 1163−1167.
(21) Dholakia Geetha, R.; Meyyappan, M.; Facchetti, A.; Marks Tobin, J. *Nano Lett.* **2006**, *6* (11), 2447−55.
(22) Kim, H. S.; Byrne, P. D.; Facchetti, A.; Marks, T. J. *J. Am. Chem. Soc.* **2008**, *130* (38), 12580−12581.
(23) Lee, K.; Lu, G.; Facchetti, A.; Janes, D. B.; Marks, T. J. *Appl. Phys. Lett.* **2008**, *92* (12), 123509/1−123509/3.
(24) Yan, H.; Yoon, M.-H.; Facchetti, A.; Marks, T. J. *Appl. Phys. Lett.* **2005**, *87* (18), 183501/1−183501/3.
(25) Hayakawa, R.; Petit, M.; Chikyow, T.; Wakayama, Y. *Appl. Phys. Lett.* **2008**, *93* (15), 153301/1−153301/3.
(26) Hong, K.; Yang, S. Y.; Yang, C.; Kim, S. H.; Choi, D.; Park, C. E. *Org. Electron.* **2008**, *9* (5), 864−868.
(27) Zhang, X.-H.; Kippelen, B. *J. Appl. Phys.* **2008**, *104* (10), 104504/1−104504/6.
(28) Huang, Q.; Evmenenko, G.; Dutta, P.; Marks, T. J. *J. Am. Chem. Soc.* **2003**, *125* (48), 14704−14705.
(29) Huang, Q.; Evmenenko, G. A.; Dutta, P.; Lee, P.; Armstrong, N. R.; Marks, T. J. *J. Am. Chem. Soc.* **2005**, *127* (29), 10227−10242.
(30) Hummelen, J. C.; Knight, B. W.; LePeq, F.; Wudl, F.; Yao, J.; Wilkins, C. L. *J. Org. Chem.* **1995**, *60* (3), 532−8.
(31) Li, C. N.; Djurisic, A. B.; Kwong, C. Y.; Lai, P. T.; Chan, W. K.; Liu, S. Y. *Appl. Phys. A: Mater. Sci. Process.* **2004**, *80* (2), 301−307.
(32) Li, C. N.; Kwong, C. Y.; Djurisic, A. B.; Lai, P. T.; Chui, P. C.; Chan, W. K.; Liu, S. Y. *Thin Solid Films* **2005**, *477* (1−2), 57−62.
(33) Yan, H.; Lee, P.; Armstrong, N. R.; Graham, A.; Evmenenko, G. A.; Dutta, P.; Marks, T. J. *J. Am. Chem. Soc.* **2005**, *127* (9), 3172−3183.
(34) Pingree, L. S. C.; Scott, B. J.; Russell, M. T.; Marks, T. J.; Hersam, M. C. *Appl. Phys. Lett.* **2005**, *86* (7), 073509−3.

in OPVs.[19,39−45] Previously, *p*-type NiO,[19] *n*-type TiO_x,[46,47] and a cross-linked $TPDSi_2$:TFB polymer blend[45] have been utilized as interfacial layers (IFLs) in the bulk-heterojunction (BHJ) OPV architecture. In the case of NiO, the addition of a thin oxide layer (10 nm) between the OPV tin-doped indium oxide (ITO) anode and the active layer blocks leakage of minority carriers (electrons) and promotes collection of majority carriers (holes), addressing problems intrinsic to the basic BHJ device design. The NiO IFL affords a 24% increase in open-circuit voltage (V_{OC}) to 638 mV and an overall increase in light-to-power conversion efficiency (*Eff*) of 70% to 5.0% with an active layer composed of poly-(3-hexylthiophene) (P3HT) and the fullerene derivative [6,6]-phenyl-C61 butyric acid methyl ester (PCBM), as compared to a bare ITO anode control device. This example also represents an ∼22% increase over the state-of-the-art device performance achievable when the IFL is conventional PEDOT:PSS (1:6 weight ratio).[48] These marked device performance enhancements clearly demonstrate the importance of OPV interfaces.

A major motivation for OPV interface research is the widely accepted shortcomings of the standard anode materials, ITO and PEDOT:PSS. Both suffer from pronounced electrical and compositional inhomogeneity.[49−51] This introduces the nontrivial problem of spatially varying work functions and limited effective interfacial area for efficient charge collection. Previous studies have addressed the effect of various organic and inorganic IFLs; however, the specific role of the ITO anode surface in OPV function has received little attention. Can it be modified in such a way that an IFL would be unnecessary? Previous reports[32,50] have shown that when ITO film surfaces are treated with aqueous haloacid solutions, the work function is increased to as high as 5.0 eV, which is accompanied by significant surface electrical homogenization. This suggests that an interface capable of Ohmic contact to the P3HT electron donor for loss-less charge collection might be realizable (Figure 1a), in addition to more effective charge collection with a greater percentage of electroactive surface area.[17,52] In this contribution, we describe the effects of aqueous HCl treatment on the surface of ITO and the consequences of incorporating HCl-treated ITO into P3HT:PCBM BHJ OPVs. Furthermore, we report that PV performance rivaling that of PEDOT:PSS-based devices can be achieved without the necessity of an IFL. To understand how this performance enhancement occurs, we probe the ITO surface as a function of HCl treatment with UV and X-ray photoelectron spectroscopy, van der Pauw electrical conductivity measurements, and topographic and conductive atomic force microscopy. Additionally, we implement a diode-based device model to further understand the effects of ITO surface treatment on device performance.

II. Experimental Section

Materials. PCBM[30] was purchased from American Dye Source, Inc. (ADS) and was further purified by several cycles of sonication in toluene followed by filtration and then sonication in pentane, followed by centrifugation. P3HT[53] was purchased from Rieke Metals, Inc., and was further purified by sequential Soxhlet extractions with methanol and hexanes. The solvent 1,2-dichlorobenzene (Drisolv) for spin-coating was purchased from EMD, distilled from P_2O_5 under anaerobic conditions, and stored under N_2. Bulk solvents (ACS grade) for substrate cleaning and HCl (concentrated) for ITO etching were purchased from EMD and used as received. PEDOT:PSS (electronic grade, 1:6 w:w) was purchased from H.C. Stark and stored in a refrigerator. LiF (99.98%) and Al slugs (99.999%) were purchased from Arcos and Sigma-Aldrich, respectively, and used as received. UV-curable ELC-2500 epoxy used for device encapsulation was purchased from Electro-lite Corp.

Instrumentation. X-ray photoelectron spectroscopy (XPS) data were collected on an Omicrometer ESCA probe (Omicrometer, Taunusstein, Germany) equipped with an EA125 energy analyzer. Photoemission was stimulated under ultrahigh vacuum (10^{-8} Torr) by a monochromated Al Kα (1486.8 eV) 300 W X-ray source with a circular spot size of ∼1.5 mm. The incident angle of the photon beam on the sample was fixed at 15° to probe only the atoms nearest the ITO surface. Binding energies of spectra are referenced to the C 1*s* binding energy set at 284.7 eV. Work functions were measured by ultraviolet photoelectron spectroscopy (UPS) using a Kratos Axis Ultra photoelectron spectrometer with a 21.2 eV He (I) excitation source and a 5 eV pass energy. The UPS spectra were collected while applying a −5.0 V sample bias to enable the identification of the low kinetic energy edge of the spectrum.

The electrical properties of the ITO films were measured with a Bio-Rad HL5500 van der Pauw measurement system. Profilometry was performed with a Tencor P-10 profilometer. Atomic force microscopy (AFM) data were generated under ambient conditions with a Veeco Dimension V AFM equipped with an Extended Tunneling AFM (TUNA) module.[54] Topographic and conductive AFM (cAFM) images were simultaneously collected in contact mode while applying a +10 mV sample bias and using a Budget Sensors ContE Cr/Pt conductive probe. An electrical connection was made to the ITO by contacting a small amount of silver paint applied to the edge of the substrate.

OPV device performance was evaluated at 298K using a Class A Spectra-Nova Technologies solar cell analyzer having a xenon light source that simulates AM 1.5G light from 400−1100 nm. The instrument was calibrated with a monocrystalline Si diode fitted with a KG3 filter to bring spectral mismatch close to unity.[48] The light source calibration standard was calibrated by the National Renewable Energy Laboratory (NREL). Four-point contacts were made to the substrate with Ag paste and copper alligator clips. Individual devices were isolated by a mask during testing to avoid light collection from adjacent devices and edge effects. Thermal stability tests were performed by heating

(35) Li, J.; Marks, T. J. *Chem. Mater.* **2008**, *20* (15), 4873−4882.
(36) Matsushima, T.; Murata, H. *J. Appl. Phys.* **2008**, *104* (3), 034507/1−034507/4.
(37) Ryu, S. Y.; Hwang, B. H.; Park, K. W.; Hwang, H. S.; Sung, J. W.; Baik, H. K.; Lee, C. H.; Song, S. Y.; Lee, J. Y. *Nanotechnology* **2009**, *20* (6), 065204/1−065204/5.
(38) Wang, F.; Qiao, X.; Xiong, T.; Ma, D. *Org. Electron.* **2008**, *9* (6), 985−993.
(39) Steim, R.; Choulis, S. A.; Schilinsky, P.; Brabec, C. J. *Appl. Phys. Lett.* **2008**, *92* (9), 093303/1−093303/3.
(40) Lee, J. K.; Coates, N. E.; Cho, S.; Cho, N. S.; Moses, D.; Bazan, G. C.; Lee, K.; Heeger, A. J. *Appl. Phys. Lett.* **2008**, *92* (24), 243308/1−243308/3.
(41) Reese, M. O.; White, M. S.; Rumbles, G.; Ginley, D. S.; Shaheen, S. E. *Appl. Phys. Lett.* **2008**, *92* (5), 053307/1−053307/3.
(42) Takahashi, K.; Suzaka, S.; Sigeyama, Y.; Yamaguchi, T.; Nakamura, J.-I.; Murata, K. *Chem. Lett.* **2007**, *36* (6), 762−763.
(43) White, M. S.; Olson, D. C.; Shaheen, S. E.; Kopidakis, N.; Ginley, D. S. *Appl. Phys. Lett.* **2006**, *89* (14), 143517/1−143517/3.
(44) Shrotriya, V.; Li, G.; Yao, Y.; Chu, C.-W.; Yang, Y. *Appl. Phys. Lett.* **2006**, *88* (7), 073508/1−073508/3.
(45) Hains, A. W.; Marks, T. J. *Appl. Phys. Lett.* **2008**, *92* (2), 023504/1−023504/3.
(46) Kim, J. Y.; Kim, S. H.; Lee, H.-H.; Lee, K.; Ma, W.; Gong, X.; Heeger, A. J. *Adv. Mater. (Weinheim, Ger.)* **2006**, *18* (5), 572−576.
(47) Kim, J. Y.; Lee, K.; Coates, N. E.; Moses, D.; Nguyen, T.-Q.; Dante, M.; Heeger, A. J. *Science (Washington, DC, U.S.)* **2007**, *317* (5835), 222−225.
(48) Shrotriya, V.; Li, G.; Yao, Y.; Moriarty, T.; Emery, K.; Yang, Y. *Adv. Funct. Mater.* **2006**, *16* (15), 2016−2023.
(49) Kemerink, M.; Timpanaro, S.; De Kok, M. M.; Meulenkamp, E. A.; Touwslager, F. J. *J. Phys. Chem. B* **2004**, *108* (49), 18820−18825.
(50) Brumbach, M.; Veneman, P. A.; Marrikar, F. S.; Schulmeyer, T.; Simmonds, A.; Xia, W.; Lee, P.; Armstrong, N. R. *Langmuir* **2007**, *23* (22), 11089−11099.
(51) Pingree, L. S. C.; MacLeod, B. A.; Ginger, D. S. *J. Phys. Chem. C* **2008**, *112* (21), 7922−7927.
(52) Jain, S. C.; Geens, W.; Mehra, A.; Kumar, V.; Aernouts, T.; Poortmans, J.; Mertens, R.; Willander, M. *J. Appl. Phys.* **2001**, *89* (7), 3804−3810.
(53) Chen, T. A.; Rieke, R. D. *J. Am. Chem. Soc.* **1992**, *114* (25), 10087−8.
(54) Leever, B. J.; Durstock, M. F.; Irwin, M. D.; Hains, A. W.; Marks, T. J.; Pingree, L. S. C.; Hersam, M. C. *Appl. Phys. Lett.* **2008**, *92* (1), 013302/1−013302/3.

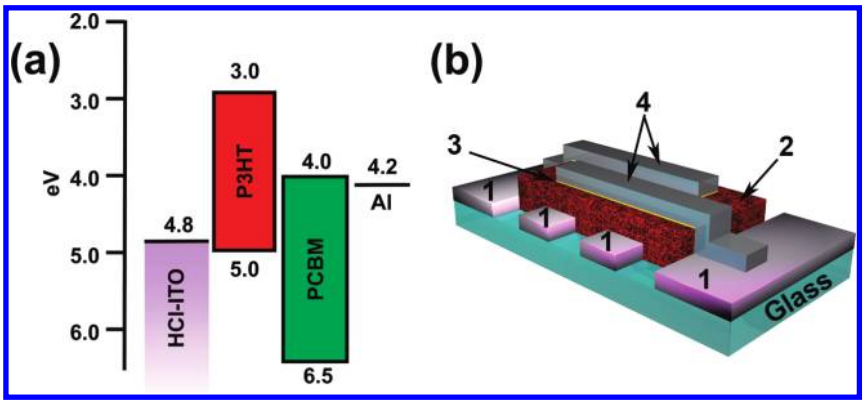

Figure 1. Depiction of (a) the energy level diagram of the present OPV devices, spatially arranged. Represented are the near-Ohmic contacts at the anode (HCl-ITO) and cathode (Al) with the HOMO of P3HT and LUMO of PCBM, respectively. Part (b) is a schematic of the OPV architecture: 1, ITO; 2, P3HT:PCBM BHJ; 3, LiF; 4, Al.

encapsulated devices at 60 °C on a hot plate in the ambient atmosphere with ambient light exposure and periodic light $J-V$ analysis.

Substrate Preparation. ITO-coated glass (11 Ω/□) was purchased from Delta Technologies, Ltd. in 25 × 75 mm strips. The substrates were patterned to make two electrically separate 3 mm anode strips and 5 mm contact strips (Figure 1b) by applying a mask and dipping in hot concentrated HCl for 10 s. The substrate was then quenched in saturated aqueous $NaHCO_3$ solution, dried with a filtered N_2 stream from a blow gun, and sonicated in hexanes at 50 °C for 30 min to remove mask adhesive. The ITO-coated glass was next cut into 25.0 × 12.5 mm substrates and cleaned by sonicating at 50 °C in aqueous detergent for 30 min, deionized (DI) water for 5 min, and then methanol, isopropanol, and acetone, sequentially, for 30 min each. The solvent-cleaned substrates were further cleaned, immediately before use, in a UV ozone (UVO) oven (Jelight Co., Inc., model 42) for 10 min under ambient atmosphere (the basis for the sample herein referred to as the "control").

PEDOT:PSS Deposition. As-received PEDOT:PSS solution was passed through 0.2 μm PTFE 13 mm syringe filters (PP casing, Whatman) onto solvent-cleaned ITO substrates treated with 30 min UVO and was then spun at 5000 rpm for 30 s. The films were annealed on a hot plate at 150 °C for 15 min in air. The coated substrates were then transferred to a glovebox immediately after annealing to minimize water condensing on the surface.

HCl ITO Treatment. In a 250 mL Erlenmeyer flask, concentrated HCl (5 mL) was combined with 195 mL of DI H_2O. The well-mixed solution was poured into a polypropylene vessel into which the ITO substrates in a polyethylene holder were then placed. The entire vessel was sonicated in a water bath between 0 and 30 min (total submersion time of ITO substrate in HCl solution) at 50 °C. Promptly after sonication, the substrate holder was removed with forceps and submerged repeatedly into fresh DI water to remove residual HCl. The substrates were subsequently dried by filtered, pressurized N_2 from a blow gun. Finally, the substrates were cleaned in the aforementioned UVO cleaner for 10 min immediately prior to use.

Device Fabrication. A clean, dry 10 mL Schlenk flask was charged with P3HT (20 mg), PCBM (20 mg), and a stir bar. The flask was cycled N_2/vacuum three times on a Schlenk line, and then purified 1,2-dichlorobenzene (1.0 mL, distilled from P_2O_5 and stored under N_2) was added under a heavy N_2 flush. The solution was then vigorously stirred for 30 min in the dark at 60 °C under a static N_2 atmosphere (closed vessel) to prevent solvent loss, and was then sonicated at 50 °C for 1 h. The active layer solution and the cleaned substrates were immediately transferred to a N_2-filled glovebox (< 1 ppm of O_2 and H_2O), and then the active layer solution was spin-coated onto bare ITO, ITO/PEDOT:PSS, and/or HCl-treated ITO anodes in sequential steps at 550 rpm for 60 s and then at 2000 rpm for 1 s (thickness = 200−220 nm). The still-wet films were immediately transferred from the spin-coater chuck to individual, covered Petri dishes and allowed to slowly dry (∼20 min) undisturbed. Electrical contact areas were then cleaned with dry, O_2-free toluene and a cotton swab, and subsequently annealed on a hot plate in the glovebox at 120 °C for 10 min. The actual annealing temperature of the films was confirmed by a thermocouple affixed to a glass slide heated under identical conditions. Still in the glovebox, LiF/Al (0.6 nm/130 nm) cathodes were next deposited sequentially, without breaking vacuum, using a thermal evaporator. The rates used were 0.1 Å/s for LiF and ∼2 Å/s for Al, with a chamber pressure of $\sim 1.0 \times 10^{-6}$ Torr. The cathodes were deposited through a shadow mask with two 2.0 mm wide rectangular apertures perpendicular to the two patterned ITO strips to create four devices per substrate (Figure 1b). Finally, the completed solar cells were encapsulated inside the glovebox with a glass slide using UV-curable epoxy, which was cured in a UV chamber for 12 min.

III. Results

The HCl-treated ITO films were characterized by AFM, cAFM, and van der Pauw measurements as well as by UPS and XPS, as discussed below. Devices fabricated from these substrates/anodes were further characterized by light and dark $J-V$ measurements. Here, we describe the effects of HCl treatment on the ITO surface and the impact of HCl-treated ITO when incorporated in P3HT:PCBM-based BHJ OPV devices. As will be presented below, optimal device performance corresponds to an HCl exposure time of 20 min, and thus this condition is the focus of the ITO surface analysis. It will be seen that this straightforward procedure modifies the electrical homogeneity, work function, and composition of the ITO surface in such a manner as to more favorably interact with the P3HT:PCBM BHJ active layer. Throughout the entirety of this investigation, the HCl-treated ITO surfaces were examined immediately after the final treatment, be it aqueous HCl or 10 min UVO, where UVO is the default treatment.

AFM/cAFM. ITO thin films are known to have a substantial grain/subgrain structure in which the latter is not observable by AFM but becomes visible when etched with haloacids.[50] These effects are also observed here with ITO grains of ca. 100−200 nm evident when the substrate is treated with UVO only, with the grain size decreasing to ca. 50 nm upon HCl + UVO treatment (Figure 2a,b). The increase in the density of features coincides with rougher films, with the rms roughness increasing from 0.80 to 1.35 nm after the HCl treatment (scan area = 4 μm^2). These changes in grain structure are also evident in the cAFM images

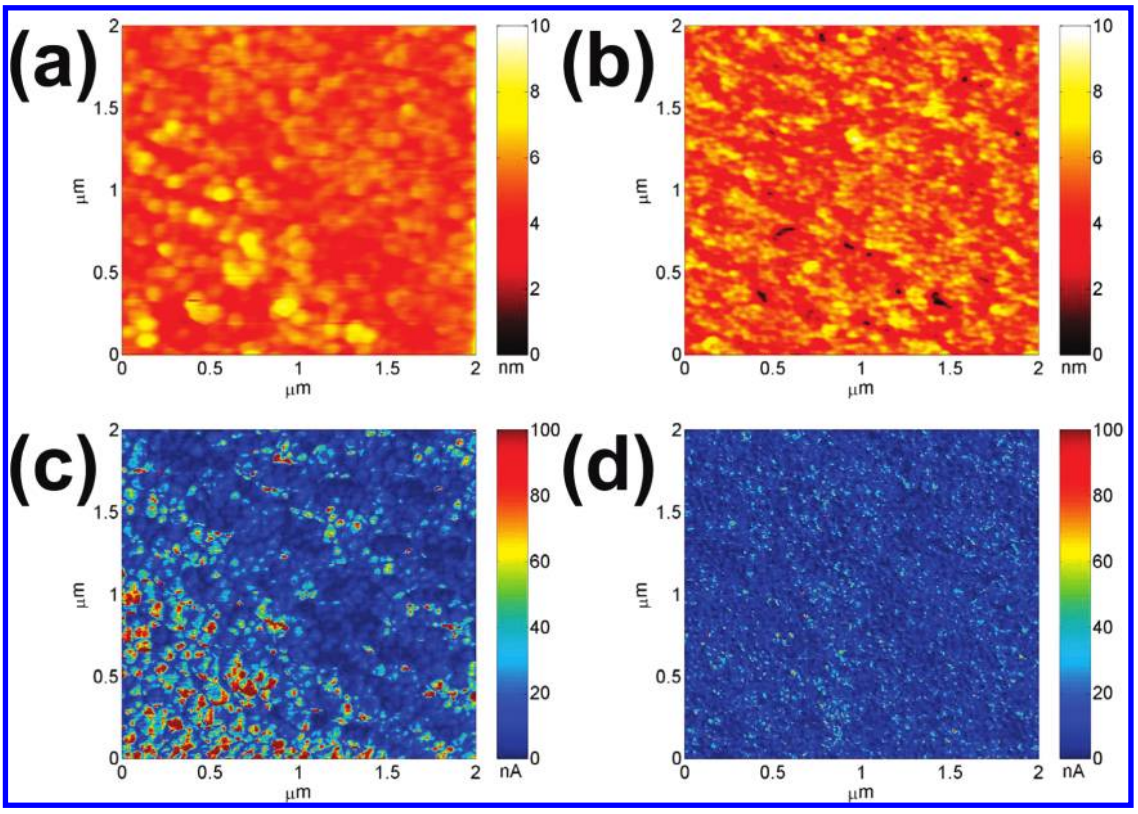

Figure 2. AFM and cAFM images of treated ITO surfaces. AFM images: (a) UVO-only treatment; (b) HCl + UVO treatment. cAFM images: (c) UVO-only treatment; (d) HCl + UVO treatment.

where grain boundaries are defined by areas of lower conductivity (Figure 2c,d). Sharply defined in the cAFM images are areas of higher conductivity, known as "hot spots", and areas of lower conductivity, known as "dead spots". When the UVO-only treated ITO is scanned at +10 mV bias, the mean current (I_{mean}) = 19.8 nA (σ = 31.1 nA, Figure 2c), and scanning under the same conditions on HCl-treated ITO yields I_{mean} = 9.11 nA (σ = 12.5 nA, Figure 2d). As seen visually when comparing parts c and d of Figure 2, an increase in surface electrical homogeneity with HCl treatment of the ITO surface is noted along with a reduction in the mean current and its standard deviation. Additionally, it is clear that the overall current is appreciably reduced by ~50% after HCl + UVO treatment, but on the macroscale, van der Pauw measurements reveal no significant change in sheet resistance (11 Ω/□).

UPS/XPS. UPS measurements reveal an increase in work function of ~0.1 eV when the ITO surface is cleaned with a combination of aqueous HCl (20 min) and UVO (10 min), in respective order, as opposed to UVO alone (Figure 3). Defining the latter as 4.7 eV,[55] the work function of the former would be 4.8 ± 0.05 eV. XPS measurements reveal a Sn:In ratio of 0.18 ± 0.05:1.0 for the solvent cleaned-only ITO surface and 0.12 ± 0.01:1.0 following HCl treatment, and these values are independent of UVO treatment (Figure 4, Table 1). A sequential reduction in C contamination with treatment is observed with an initial C:In ratio of 2.37 ± 0.12:1.0 for untreated ITO to 0.36 ± 0.02:1.0 with solvent treatment. Ten minutes of UVO treatment further reduces the C:In ratio to 0.23 ± 0.01:1.0, and the respective combination of HCl treatment and 10 min UVO also yields 0.23 ± 0.01:1.0, remarkably similar to an ITO surface treated with RIE/

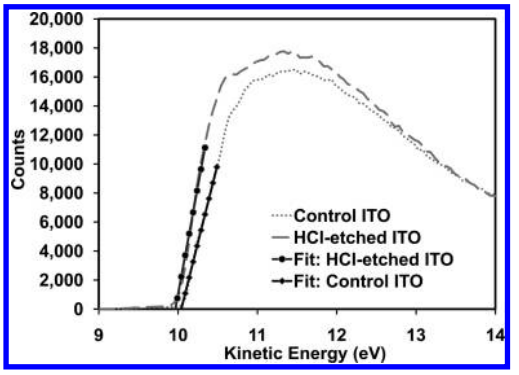

Figure 3. UPS spectra of an ITO surface treated with UVO only ("control ITO") or HCl + UVO ("HCl-etched ITO"; exposure times: HCl = 20 min, UVO = 10 min). Since both the HCl-etched and UVO-only processed ITO samples share a common Fermi edge, only the part of the UPS spectrum that includes the low kinetic energy edge of each sample is depicted. To determine the low-energy edge, a linear curve was fit to the initial 60% of the points in the leading edge of each spectrum.

oxygen plasma. Additionally, the O:In ratio is 1.20 ± 0.06:1.0 with solvent cleaning only and 1.12 ± 0.06:1.0 in combination with 10 min UVO. HCl treatment reduces this ratio to 1.06 ± 0.05:1.0, and subsequent 10 min UVO treatment further decreases the ratio to 1.03 ± 0.05:1.0. Chloride or other metallic contaminants are not detected by XPS.

OPV Device Characterization. After initial optimization of the aqueous HCl solution concentration to 0.95% (~0.3 M) and UVO exposure time to 10 min, the optimum ITO exposure time to HCl was determined. The ITO substrates were submerged in the aqueous HCl solution and sonicated for durations between 0 and 30 min (total submersion time), and then were further treated in

(55) Sugiyama, K.; Ishii, H.; Ouchi, Y.; Seki, K. *J. Appl. Phys.* **2000**, *87* (1), 295−298.

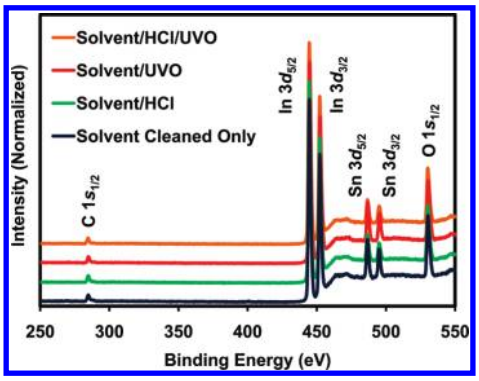

Figure 4. Offset XPS spectra for four ITO surface treatments. All data are normalized to the In $3d_{5/2}$ peak of the "solvent/HCl/UVO" sample. Note the decrease in the Sn:In and O:In ratios with additional treatment.

Table 1. Atomic Ratios Determined from the XPS Data Stated in Each Column As Compared to the In $3d_{5/2}$ Peak for ITO Thin Film Surfaces As-Received (Untreated) or Treated by Solvent Cleaning, Solvent/UVO, Solvent/HCl, and Solvent/HCl/UVO in Respective Order[a]

substrate	C $1s_{1/2}$	O $1s_{1/2}$	Sn $3d_{5/2}$
untreated ITO	2.37 ± 0.12	1.96 ± 0.10	0.16 ± 0.01
solvent-cleaned ITO	0.36 ± 0.02	1.20 ± 0.06	0.18 ± 0.01
solvent/UVO	0.23 ± 0.01	1.12 ± 0.06	0.18 ± 0.01
solvent/HCl	0.27 ± 0.01	1.06 ± 0.05	0.12 ± 0.01
solvent/HCl/UVO	0.23 ± 0.01	1.03 ± 0.05	0.12 ± 0.01

[a] HCl exposure time = 20 min, UVO = 10 min.

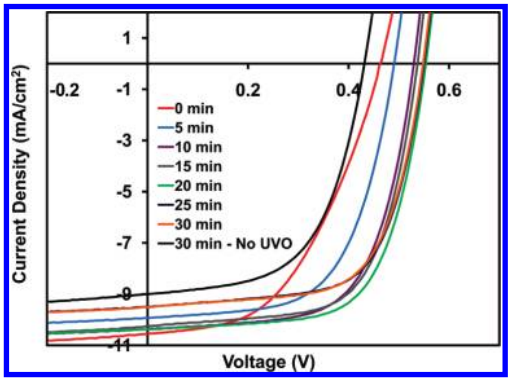

Figure 5. Light $J-V$ data for BHJ OPV devices (glass/ITO/P3HT:PCBM/LiF/Al) containing ITO anodes with the indicated aqueous HCl solution exposure times, followed by 10 min UVO treatment. An additional plot is included for an ITO substrate that received 30 min of HCl solution exposure time but not the subsequent UVO treatment (black line). Data at 25 min HCl exposure time are indistinguishable from by data at 30 min HCl exposure time.

the UVO oven for 10 min. The completed devices were of the structure glass/ITO/P3HT:PCBM/LiF/Al. Light $J-V$ data reveal a progressive rise then decline of V_{OC} and fill factor (FF) with maxima reached after 20 min HCl exposure time and with metrics of 554 mV and 66%, respectively (Figure 5). An initial drop in J_{SC} is noted on HCl treatment, with a gradual rise in value to a maximum at 15−20 min exposure time. An additional substrate at 30 min HCl exposure time, but without subsequent UVO treatment, was also included in these experiments to gauge the effects and necessity of UVO. When compared to the corresponding ITO substrate treated with HCl + UVO, precipitous declines in V_{OC}, J_{SC}, and FF values are observed. OPV device response data are summarized in Table 2.

Table 2. Summary of the Performance Parameters from the Light $J-V$ Data for BHJ OPV Devices of the Structure Glass/ITO/P3HT:PCBM/LiF/Al[a]

exposure time (min)	V_{OC} (V)	J_{sc} (mA/cm^2)	FF (%)	Eff (%)
0	0.463	10.6	48.6	2.38
5	0.491	9.93	61.0	2.97
10	0.531	10.2	65.5	3.54
15	0.537	10.4	64.6	3.59
20	0.554	10.4	65.7	3.77
25	0.550	9.50	65.6	3.43
30	0.549	9.51	65.3	3.41
30[b]	0.432	8.99	57.6	2.24
40 nm PEDOT:PSS	0.583	10.1	64.8	3.81

[a] Additional data are included for a device of the structure glass/ITO/40 nm PEDOT:PSS/P3HT:PCBM/LiF/Al for reference. [b] Sample treated with HCl for 30 min but without postetch UVO treatment.

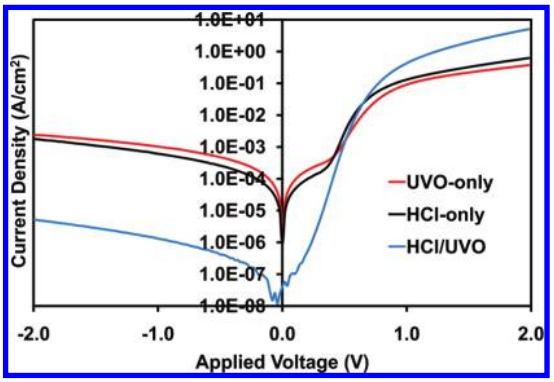

Figure 6. Dark $J-V$ data plots of glass/ITO/P3HT:PCBM/LiF/Al BHJ OPV devices incorporating ITO anodes treated with UVO only, aqueous HCl only, and finally HCl then UVO. The combination of surface treatments yields dramatic decreases in reverse-bias current and a smaller increase in forward-bias current. The current at $V = 0.0$ for the HCl + UVO sample is outside the sensitivity range of the sourcemeter (Keithley model 2400).

Dark $J-V$ device data are compared for ITO substrates treated with UVO-only, HCl-only, and HCl + UVO (HCl etch time = 30 min) in Figure 6. Scans were taken from −2.0 to +2.0 V, and the device area-normalized data are plotted on a logarithmic scale. Devices having substrates treated with only UVO or only HCl exhibit similar response, although the HCl-only devices show slightly less current in the negative quadrant and slightly greater current in the positive quadrant, with rectification ratios of ~10^2 for both device types. When both treatments are combined (HCl and then UVO), the rectification ratio increases substantially to 10^6 and the current at $V = 0.0$ is below the sensitivity of the sourcemeter (Keithley model 2400). The current in the negative voltage quadrant is reduced by ~$10^3\times$ and increased by ~$10^1\times$ in the positive voltage quadrant. On the basis of a least-squares fit of the dark data (Figure 6), series resistance (R_S) values were calculated to be 3.13, 2.52, and 0.79 Ω·cm^2 for UVO-only, HCl-only, and HCl-UVO, respectively.

In testing device temporal stability, devices based on HCl-treated ITO (stored in a glovebox) were periodically evaluated for performance, and the metrics were found to be within ±5% of their original values after 11 months. The time span is only limited by the date of this writing. To evaluate device thermal stability, PEDOT:PSS-based and HCl-treated ITO-based devices were continuously heated at 60 °C in the ambient atmosphere on a hot plate and tested periodically over 1000 h. For both device types, there is an initial drop in power output over the first 20 h, followed by a linear regime ($R^2 > 0.99$) with a gradual decline.

Table 3. Parameters Extracted from a Least-Squares Fit of the Dark $J-V$ Plots in Figure 6 to Eq 1

substrate	R_S ($\Omega\cdot cm^2$)	n	R_{Sh} ($\Omega\cdot cm^2$)	J_0 at 320 K (A/cm^2)	V_{OC}, measured (V)	V_{OC}, calculated (V)
HCl-UVO	0.79	1.90	2.14×10^6	3.26×10^{-7}	0.549	0.539
HCl-only	2.52	1.84	1.31×10^6	5.08×10^{-7}	0.432	0.495
UVO-only	3.13	2.15	1.36×10^3	6.67×10^{-7}	0.463	0.573

The linear portion of the data was then extrapolated to zero power output to estimate time for device failure. It was found that after ~1200 h the PEDOT:PSS-based devices fail, while HCl-treated ITO-based devices remain within ~75% of their original power output. The latter were found to fail after ~4700 h.

OPV Device Modeling. Finally, given the variation in V_{OC} with the different ITO treatments, V_{OC} analyses were performed based upon a well-established single diode model:[56−64]

$$V_{OC} = n\frac{k_B T}{e}\ln\left[1+\frac{J_{ph}}{J_0}\left(1-\frac{V_{OC}}{J_{ph}R_{Sh}}\right)\right] \quad (1)$$

where n is the diode ideality factor, k_B Boltzmann's constant, T temperature, e the elementary charge, J_{ph} the photocurrent generated by the cell before recombination losses, J_0 the reverse saturation current, and R_{Sh} the shunt resistance. Prior studies have applied eq 1 to calculate accurate values of V_{OC}. Here, the parameters in eq 1 were determined by a least-squares fit of the dark data (Figure 6) for the HCl/UVO, HCl-only, and UVO-only cases (assuming T = 298 K for the dark conditions). Table 3 summarizes these results. Methods reported by Perez et al.[57] and Potscavage et al.[58] were used to estimate the temperature dependence of J_0, and (assuming T = 320 K under illumination) V_{OC} values were calculated to be 0.54 V for HCl-UVO, 0.57 V for UVO-only, and 0.50 V for HCl-only. Note that for the UVO-only and HCl-only cases there is significant deviation between the calculated and measured V_{OC} values, but for the HCl-UVO case, the calculated and measured values are nearly identical (0.54 V vs 0.55 V, respectively).

IV. Discussion

The electronic structural properties and performance effects of anode interfacial layers in organic-based diodes such as OLEDs[33] and OPVs[19,45] have been major research foci in this laboratory and elsewhere. The phenomena underlying the effects of interlayers on OPV performance are presently not well-understood, but the goals motivating the investigations are: (i) creation of an Ohmic contact for the unhindered extraction of charge, (ii) providing a high-lying conduction band (CB)/lowest unoccupied molecular orbital (LUMO−in the case of the anode) to prevent minority charge (electron) collection and consequent counterdiode formation, (iii) suppressing leakage current,[17] and (iv) thermally stabilizing the interface with respect to degradation/decohesion.[28,29,35,45] The consequences of an effective electron-blocking layer (EBL) on $J-V$ metrics are anticipated to be increased V_{OC} due to reduction in counter bias,[18,65−67] increased J_{SC} with increased hole conductivity reflecting the Ohmic contact and reduced interfacial charge trap densities,[68] and increased FF due to reduced R_S and increased R_{Sh}.[69] Indeed, such effects are observed, and enhanced performance metrics achieved, when IFLs of the cross-linked TPDSi$_2$:TFB[45] polymer blend and p-NiO[19] are introduced into MDMO-PPV-based and P3HT-based BHJ devices, respectively. PEDOT:PSS is also used extensively as an IFL with both of these OPV materials systems.[70,71] Each interfacial material offers the appropriate energy levels to serve the intended purpose, while having a sufficient bandgap to remain transparent in the regions where the BHJ spectral response is greatest. While successful, these approaches introduce the complexity of an additional fabrication step to incorporate the IFL and the synthesis/purification of the requisite IFL materials. The optimized modification of the ITO surface with dilute aqueous HCl solutions reported here achieves performance metrics comparable to devices containing a PEDOT:PSS IFL, but in a simpler fabrication process and with greater device stability.

The optimized ITO anode surface treatment includes traditional solvent cleaning of the ITO substrate, followed by sonication in 0.95% (~0.3 M) HCl solution for 20 min at 50 °C, rinsing in DI water, and finally UVO treatment for 10 min. The result is Eff = 3.77% at 25 °C and 1000 W/m^2 AM 1.5G irradiation. This power conversion efficiency is approximately equal to that of a device fabricated in parallel with a PEDOT:PSS IFL (Table 2). When compared to a device that contains ITO prepared only by traditional solvent cleaning and UVO treatment (the control), the V_{OC} is increased 20% from 463 to 554 mV, FF is increased 35% from 49 to 66%, and Eff is increased 59% from 2.38 to 3.77%. J_{SC} remains within 2% of the value of the former device. Changes in the dark $J-V$ data are equally substantial with an increase in rectification ratio from 10^2 to 10^6. Interestingly, the dark data are nearly identical for devices containing either HCl-treated ITO (no UVO treatment) or UVO-treated ITO anodes, although the HCl-treated ITO-based devices are slightly superior. It is not until the two treatments are combined that substantial performance increases are observed (the same trend is true in the light $J-V$ data). With HCl + UVO-treated ITO, the reverse-bias current drops 10^3x at −2.0 V and forward-bias current density increases 10^1x at +2.0 V, indicating considerably suppressed leakage current and reduced R_S. As shown in Table 3, R_S drops significantly for the HCl-UVO case: R_S = 0.79 $\Omega\cdot cm^2$ for the HCl-UVO treatment versus R_S = 3.1 and 2.5 $\Omega\cdot cm^2$ for the UVO-only and HCl-only treatments, respectively. Moreover, the decreased

(56) Huynh, W. U.; Dittmer, J. J.; Teclemariam, N.; Milliron, D. J.; Alivisatos, A. P.; Barnham, K. W. J. *Phys. Rev. B* **2003**, *67* (11), 12.
(57) Perez, M. D.; Borek, C.; Forrest, S. R.; Thompson, M. E. *J. Am. Chem. Soc*. **2009**, *131* (26), 9281−9286.
(58) Potscavage, W. J.; Yoo, S.; Kippelen, B. *Appl. Phys. Lett*. **2008**, *93* (19).
(59) Schilinsky, P.; Waldauf, C.; Hauch, J.; Brabec, C. J. *J. Appl. Phys*. **2004**, *95* (5), 2816−2819.
(60) Shockley, W. *Bell Syst. Tech. J*. **1949**, *28* (3), 435−489.
(61) Yoo, S.; Domercq, B.; Kippelen, B. *J. Appl. Phys*. **2005**, *97* (10).
(62) Sze, S. M. *Physics of Semiconductor Devices*: Wiley-Interscience: New York, 1981.
(63) Servaites, J. D.; Ratner, M. A.; Marks, T. J. *Appl. Phys. Lett*. **2009**, *95*, 163302.
(64) Servaites, J. D.; Yeganeh, S.; Ratner, M. A.; Marks, T. J. *Adv. Funct. Mater*. **2009**, *19*, 1−8.
(65) Mutolo, K. L.; Mayo, E. I.; Rand, B. P.; Forrest, S. R.; Thompson, M. E. *J. Am. Chem. Soc*. **2006**, *128* (25), 8108−8109.
(66) Xue, J.; Rand, B. P.; Forrest, S. R. *Proc. SPIE - Int. Soc. Opt. Eng*. **2006**, *6334* 63340K/1−63340K/10.
(67) Fortunato, E.; Ginley, D.; Hosono, H.; Paine, D. C. *MRS Bull*. **2007**, *32* (3), 242−247.
(68) Mandoc, M. M.; Kooistra, F. B.; Hummelen, J. C.; de Boer, B.; Blom, P. W. M. *Appl. Phys. Lett*. **2008**, *91* (26), 263505/1−263505/3.
(69) Dadu, M.; Kapoor, A.; Tripathi, K. N. *Sol. Energy Mater. Sol. Cells* **2001**, *69* (4), 353−359.
(70) Li, G.; Shrotriya, V.; Huang, J.; Yao, Y.; Moriarty, T.; Emery, K.; Yang, Y. *Nat. Mater*. **2005**, *4* (11), 864−868.
(71) Wienk, M. M.; Kroon, J. M.; Verhees, W. J. H.; Knol, J.; Hummelen, J. C.; van Hal, P. A.; Janssen, R. A. J. *Angew. Chem., Int. Ed*. **2003**, *42* (29), 3371−3375.

current at ±0.0 V indicates a significant increase in the device shunt resistance R_{Sh} consistent with the large increases in *FF* and V_{OC} observed in the light data. A least-squares fit of the dark data verifies this to be true with an ~60% increase in R_{Sh} (Table 3).

A key motivation for investigating the effects of incorporating HCl-treated ITO into P3HT:PCBM BHJ devices is that the HCl treatment is known to increase the ITO work function from 4.7 eV, with UVO or O_2 plasma treatment only, to close to 5.0 eV with the combination of HCl and UVO (or O_2 plasma treatment).[31,32,50] This is beneficial since an Ohmic contact would now be possible with the HOMO of P3HT, assuming a constant vacuum energy level (E_{vac}). An Ohmic contact would promote more efficient charge (hole) collection without energy loss or a Schottky barrier. Here, the UPS measurements reveal a work function increase of ~0.1 eV when the ITO surface is treated with HCl + UVO, for a final value of 4.8 ± 0.01 eV. Although not exactly Ohmic, a constant E_{vac} is tentatively assumed, and its adjustment could compensate for the remaining energy difference (+0.2 eV) to match that of the P3HT HOMO energy (5.0 eV). These issues are discussed further below.

The origin of acid-induced changes in the ITO work function has been discussed previously,[31,32,50,55] and it appears from the present results that the observed reduction in the Sn:In ratio (0.18 ± 0.01:1.0 with UVO treatment only and 0.12 ± 0.01:1.0 with HCl treatment, with or without UVO treatment) depresses the Fermi energy (E_f).[72] XPS also reveals that the O:In ratio is reduced from a ratio of 1.20 ± 0.06:1.0 with solvent cleaning or in combination with UVO to 1.06 ± 0.05:1.0 with HCl treatment, and with successive UVO treatment, the ratio further decreases to 1.03 ± 0.05:1.0. The dependence of surface [O] on the work function of ITO is unclear, with conflicting reports. When H_2O_2 is used to treat the ITO surface,[73] Kugler et al. observe results similar to this report (i.e., a decrease in O:In with an increase in work function after oxidative treatment). In contrast, when H_3PO_4 is used to treat the surface, the reverse (i.e., increase in O:In with an increase in work function) is observed.[74] However, H_3PO_4 surface adsorption was also observed, and this would artificially increase O:In. In the present work, no Cl was detected on the ITO surface. Nonstoichiometric ITO surfaces with O:In as low as 0.8:1.0 have been reported,[75] and they result in a charged film surface, which can have multiple implications. First, the resultant charge/chemical depletion layer is additionally responsible for the shift in E_f toward the valence band and the subsequent increase in work function. Second, a charged ITO surface would create an interfacial dipole with the organic active layer shifting E_{vac}, potentially accommodating the present Ohmic contact observed in the $J-V$ data.[76−80] Third, such a surface may have an enhanced interfacial dipole−dipole interaction with the P3HT and PCBM active layer components, in accord with the enhanced device thermal stability (see Results section).

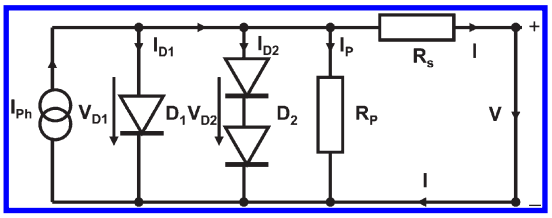

Figure 7. Equivalent circuit diagram for an OPV device where the photocurrent (I_{Ph}) is in parallel with D_1, the principal diode. Two diodes shown in series (for diagram simplicity, D_2), representing multiple parasitic recombination pathways, are also each in parallel with I_{Ph}. Also present are a parallel resistor (R_P, otherwise known as R_{Sh}) and a series resistor (R_S).

The compositional/electrical homogeneity of the anode surface has important implications for OPV device performance. A heterogeneous near-surface composition is known to create a multitude of surface states,[17,50,68] which act as parasitic recombination centers, introducing additional diodes into the OPV device equivalent circuit (D_2, Figure 7) in addition to the primary diode (D_1, Figure 7), and consequently reducing V_{OC} and increasing J_0. Such a surface is observed here with UVO-only cleaned ITO anode surfaces, with the presence of "hot spots", peaks of enhanced electrical conductivity, and "dead spots", troughs of electrical resistivity clearly evident in the cAFM images (Figure 2c). The source of the hot and dead spots has been attributed to the uneven distribution of Sn across the surface (where hot spot = high [Sn], dead spot = low [Sn]) and C contamination.[50] When ITO surfaces are subjected to HCl + UVO treatment, there is a marked reduction in C contamination and the Sn:In ratio, which accompanies the electrical homogenization and reduced conductivity of the ITO surface (UVO-only treated ITO: I_{mean} = 19.8 nA, σ = 31.1 nA, Figure 2c; HCl-treated ITO: I_{mean} = 9.11 nA, σ = 12.5 nA, Figure 2d). Note that a reduction in the O:In ratio (as observed here) corresponds to a reduction in surface conductivity.[75] The reduction in surface state density with surface homogenization is supported by the observed increases in V_{OC} and R_{Sh} and a reduction in R_S (Table 3). These observations are significant in that they provide additional understanding of the mechanism of OPV performance enhancement on IFL introduction, in addition to the previously established models invoking EBL function.[17,19]

When an IFL is introduced into the glass/ITO/IFL/P3HT:PCBM/LiF/Al device structure, where IFL = PEDOT:PSS or *p*-NiO, V_{OC} increases to between 575−600 and 600−640 mV, respectively, as opposed to the 554 mV reported here for HCl-treated ITO (other increases in OPV performance metrics are comparable or superior to those accompanying the introduction PEDOT:PSS or *p*-NiO). In addition to electron collection at the anode−the suppression of which is the primary role of an EBL−it can be concluded from the present information that surface states that impede/destroy charge carriers play a substantial role in limiting device performance by hindering hole collection. Finally, the accuracy of eq 1 in modeling V_{OC} for the HCl-UVO case, while providing relatively inaccurate estimates for the HCl-only and UVO-only cases, supports the conclusion that the HCl-UVO treatment indeed creates a uniform ITO surface relative to the other two cases. The variations in the ITO surface for the HCl-only and UVO-only treatments allows for additional recombination pathways and more complex charge injection dynamics at the ITO interface, thereby requiring a more complex modeling approach beyond the single diode approach represented

(72) Harvey, S. P.; Mason, T. O.; Gassenbauer, Y.; Schafranek, R.; Klein, A. *J. Phys. D: Appl. Phys*. **2006**, *39* (18), 3959−3968.
(73) Kugler, T.; Johansson, Å.; Dalsegg, I.; Gelius, U.; Salaneck, W. R. *Synth. Met*. **1997**, *91* (1−3), 143−146.
(74) Nuesch, F.; Rothberg, L. J.; Forsythe, E. W.; Toan Le, Q.; Gao, Y. *Appl. Phys. Lett*. **1999**, *74* (6), 880−882.
(75) Neubert, T.; Neumann, F.; Schiffmann, K.; Willich, P.; Hangleiter, A. *Thin Solid Films* **2006**, *513* (1−2), 319−324.
(76) Hatton, R. A.; Willis, M. R.; Shannon, J. M. *Chem. Phys. Lett*. **2007**, *434* (1−3), 82−85.
(77) Kawabe, E.; Yamane, H.; Sumii, R.; Koizumi, K.; Ouchi, Y.; Seki, K.; Kanai, K. *Org. Electron*. **2008**, *9* (5), 783−789.
(78) Nakano, Y.; Yanagisawa, S.; Hamada, I.; Morikawa, Y. *Surf. Interface Anal*. **2008**, *40* (6−7), 1059−1062.
(79) Zhang, W.; Gao, B.; Yang, J.; Wu, Z.; Carravetta, V.; Luo, Y. *J. Chem. Phys*. **2009**, *130* (5), 054705/1−054705/5.
(80) Graham, A. L.; Yang, X.; Alloway, D. M.; Wysocki, V. H.; Lee, T. R.; Lee, P. A.; Armstrong, N. R. *Abstracts of Papers*, 230th ACS National Meeting, Washington, DC, Aug 28−Sept. 1, 2005 **2005**, COLL-327.

in eq 1 (e.g., see circuit diagram in Figure 7). The HCl-UVO treatment, on the other hand, removes these recombination complexities and is accurately modeled by a single diode description.

V. Conclusions

This contribution examines the effect of aqueous HCl treatment on the surface of ITO films and its implications for the performance of BHJ OPVs having the structure glass/ITO/P3HT:PCBM/LiF/Al. Under optimized HCl + UVO treatment, the ITO surface chemistry evidences reduced Sn:In and O:In ratios, greater surface compositional and electronic homogeneity, and a charged surface. The homogenization of the ITO surface results in reduced charge trap density, yields improved V_{OC} and *FF* parameters, and is accurately modeled through a simplified single diode approach. These results provide insight into the mechanism by which an IFL enhances OPV performance, in addition to the IFL function as a simple EBL. The HCl treatment is sensitive to solution concentration, exposure time, and post-treatment−surface chemistry, and light and dark device response are all affected by post-treatment with UVO. Device performance with an optimized HCl + UVO-treated ITO electrode greatly enhances the device *Eff* from 2.38% for the control device to 3.77%, essentially equaling the performance of a device with a PEDOT:PSS IFL but with improved long-term temporal and thermal stability. Such a result shows that for optimum OPV device performance, simple chemical modification of the anode surface can achieve many of the same effects as an interfacial layer, but with significantly simplified device fabrication.

Acknowledgment. We thank BP Solar, the AFRL Materials & Manufacturing Directorate, the DOE (DE-FG02-06ER46320), the Army Research Office (ARO W911NF-05-1-0177), and the NSF (ECS-0609064) for support of this research. We thank the NSF-MRSEC program through the Northwestern Materials Research Center (DMR-0520513) for support of characterization facilities. We thank Dr. D. B. Buchholz for many useful discussions.